Supporting materials for

Selective Excitation Doubles the Transfer Of Parahydrogen-Induced Polarization To Heteronuclei

Andrey. N. Pravdivtsev[†]***, *Frowin Ellermann*[†], *Jan.-Bernd Hövener*

Section Biomedical Imaging, Molecular Imaging North Competence Center (MOIN CC), Department of Radiology and Neuroradiology, University Medical Center Kiel, Kiel University, Am Botanischen Garten 14, 24118, Kiel, Germany

Contents

1. Methods and experiments

Simulations. We used an in-house written Matlab script to simulate phINEPT+ and s90-phINEPT+, which uses the magnetic resonance open source initiative (MOIN) spin library.[1] The library was already successfully applied to simulate SLIC-SABRE experiments.[2] The code, including a description and various examples, is available online[3] and in SI.

Spectrometer. All NMR spectra were acquired using a 400 MHz WB NMR spectrometer (Avance Neo, Bruker) and a 5 mm BBO NMR probe (Bruker).

pH_2 generator. Hydrogen gas with a 50 % fraction of pH_2 was prepared at 30 bar and stored in a 1 L aluminum cylinder using an in-house-built and designed pH_2 generator.[4]

Bubbling system. There are three major regimes in the operation of the pH_2 bubbling system (**Fig. S1**): pressurization (1), bubbling (2), and release (3), controlled automatically or manually with three solenoid valves: hydrogen input valve (H2V), by-pass valve (BPV), and pressure release valve (PRV). The complete part number list of all components is available in **Tab S1** with a Brutto cost of 4,200 Euro. A video demonstration is provided in supporting materials.

- **Pressurization.** *H2V, BPV: opened, PRV: closed.*

Initially, there is no gas in the system (ambient pressure). The H2V valve opened right after BPV resulting in the system pressurization within 1-2 seconds to the desired value (6.9 bar = 100 psi in our case). BPV has to be opened to ensure equal pressure on the inflow and outflow side from the NMR tube. A mass-flow controller (MFC) ensured slow pressurization. We observed only a few tiny bubbles in the NMR tube with a flow rate of 35 sccm (standard cubic centimeters per minute) set by the MFC. The system pressure was controlled and adjusted with a pressure regulator (PR) and a backpressure unit (BP). It is essential to keep the PR value slightly above BP, such that gas flushing is possible without wasting too much gas.

- **Bubbling.** *H2V: opened. PRV, BPV: closed.*

When the system was pressurized, the closing of BPV resulted in a slow inflow of hydrogen in the NMR tube. Again, the MFC controlled the speed of the bubbling and was kept at a constant 35 sccm.

- **Release.** *BPV, PRV: opened, H2V: closed.*

When the experiment was over, or there was another need to release the pressure, e.g., to inject the saline solution, the pressure was relieved. To do so, H2V should be closed, and BPV and PRV should be opened. The flow regulator, which stays right after the PRV, ensures a steady release of the gas pressure and prevents splashes or the uncontrolled rise of the liquid column in the NMR tube.

Chemistry. Vinyl acetate (VA, CAS 108-05-4, V1503, Sigma Aldrich), 1,4-Bis[(phenyl-3-propanesulfonate) phosphine] butane disodium salt – [Rh] (717347, Sigma Aldrich), chloroform-d 99.8% (00405, Deutero GmbH) were used without additional purification. All experiments were carried out in a single short reaction. The NMR tube contained 450 μL chloroform-d with 10 mM [Rh], and 20 mM VA. A complete (100%) hydrogenation of VA to EA is reached after $\tau_b = 7$ s including pressurization and the bubbling stage.

NMR tube. For the high-pressure experiments, gas-tight middle-wall NMR tubes (524-PV-7, Wilmad-LabGlas) with a modified screw cap were used. We made a hole in the cap and put two

PEEK capillaries (1/32” OD, 0.005” ID, Part num. 1576, IDEX) through. Then it was all glued together with a 2-component glue (Loctite 3090, Henkel).

Polarization. Polarization and multiplet polarization were calculated as it is detailed in SI.

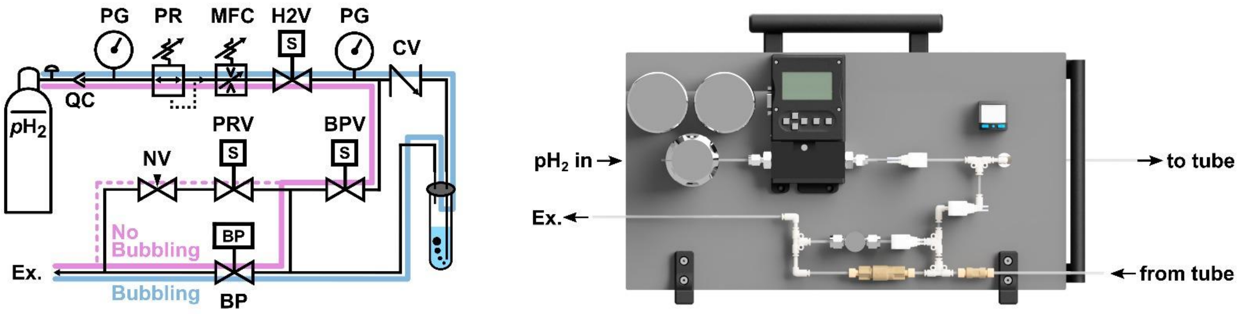

Figure S1. Scheme (A) and 3D rendering (B) of the pH_2 bubbling setup. The parahydrogen supply was connected to the setup using a quick-connector (QC). A regulator (PR) was used to set the desired pressure (0-10 bar). A mass-flow controller (MFC) was used to set the flow rate. Three solenoid valves, either controlled manually or by the spectrometer, were used to direct the flow of hydrogen: hydrogen input valve (H2V), by-pass valve (BPV), and pressure release valve (PRV). The other components of the system are a needle valve (NV), a check valve (CV), a backpressure valve (BP), and pressure gauges (PG). The list of all components is given in **Tab S1**.

The photo of up to 10 bar H_2 bubbling system (**Fig S1,S2**) and all essential components (**Tab S1**) are given here to facilitate the development of PHIP.

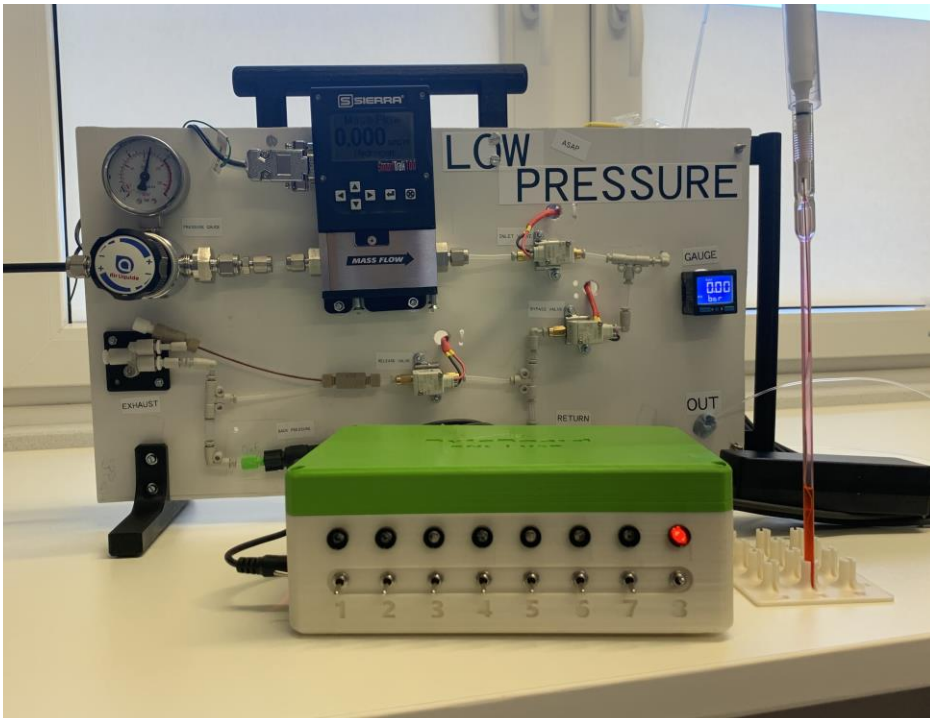

Figure S2. Photo of the up to 10 bar pH_2 bubbling setup, which scheme and rendering are shown in Fig S1. The video of the system performance is available as an additional video file.

Table S1. Complete list of components used to construct the pH_2 bubbling system with approximate prices.

№	Name	Amount	Price, incl. VAT (Euro/unit)	Price, incl. VAT (Euro)
General				
1	Massflow-Controller [Sierra Instruments], C100L-DD-1-OV1-SV1-PV2-V1-S0-C0 100-T8D(EU) 100-CRN	1	2,202.69	2,202.69
2	Pressure regulator [AirLiquide], BS50-10-3 5	1	251.09	251.09
3	Selenoid-Valve [SMC], VDW10AA	3	20.15	60.45
4	M5 to 3.2mm Adapter [SMC], KQ2H23-M5A	7	1.82	12.74
5	5mm Pressure/Vacuum NMR Tube [Wilmad], 524-PV-7	1	230.37	230.37
6	Pressure gauge [Festo], SPAN-P10R-M5F-PNLK-PNVBA-L1	1	113.95	113.95
7	T-piece 3.2mm [SMC], KQ2T23-00A	5	3.81	19.05
8	L-piece 3.2mm [SMC], KQ2L23-04A	5	2.76	13.80
9	PEEK Union 1/16 [IDEX], P-702	2	23.07	46.14
10	PEEK Union 1/8 [IDEX], P-703	2	23.07	46.14
11	Needle valve [Swagelok], SS-SS2-VH	1	241.59	241.59
12	Check valve inline [IDEX], P-696	1	145.11	145.11
13	BPR Assembly 100 psi [IDEX], P-787	1	110.93	110.93
14	Quick connect stem [Swagelok], SS-QC4-D-6M0	1	51.05	51.05
15	Adapter 6mm to 1/8” [Swagelok], SS-200-R-6M	1	14.77	14.77
16	Adapter 6mm to G3/8” [Swagelok], SS-6M0-1-6RS	2	21.36	42.72
17	6mm tube 3m [AS-Drucklufttechnik], PA 6X3 HD SCHWARZ	1	3.93	3.93
18	Microtight adapter 1/16” x 1/32”, PEEK, RED [IDEX], P-881	2	58.08	116.16
Tubing (Prices are given for packaging size, only fraction was used)				
19	PEEK Tubing 360 µm x 150 µm x 5’, Yellow [IDEX], 1572	1	77.64	77.64
20	PEEK Tubing Orange 1/32” OD x .020” ID x 5ft, [IDEX], 1569	1	53.01	53.01
21	PFA Tubing Natural 1/16” OD x .040” ID x 50ft [IDEX], 1507L	1	125.64	125.64
22	PFA Tubing Natural 1/8” OD x 1/16” ID x 50ft [IDEX], 1509L	1	209.30	209.30
Total price for the complete set incl. tools and gases, incl. 19 % VAT				**4,188.27**

2. Relaxation after INEPT

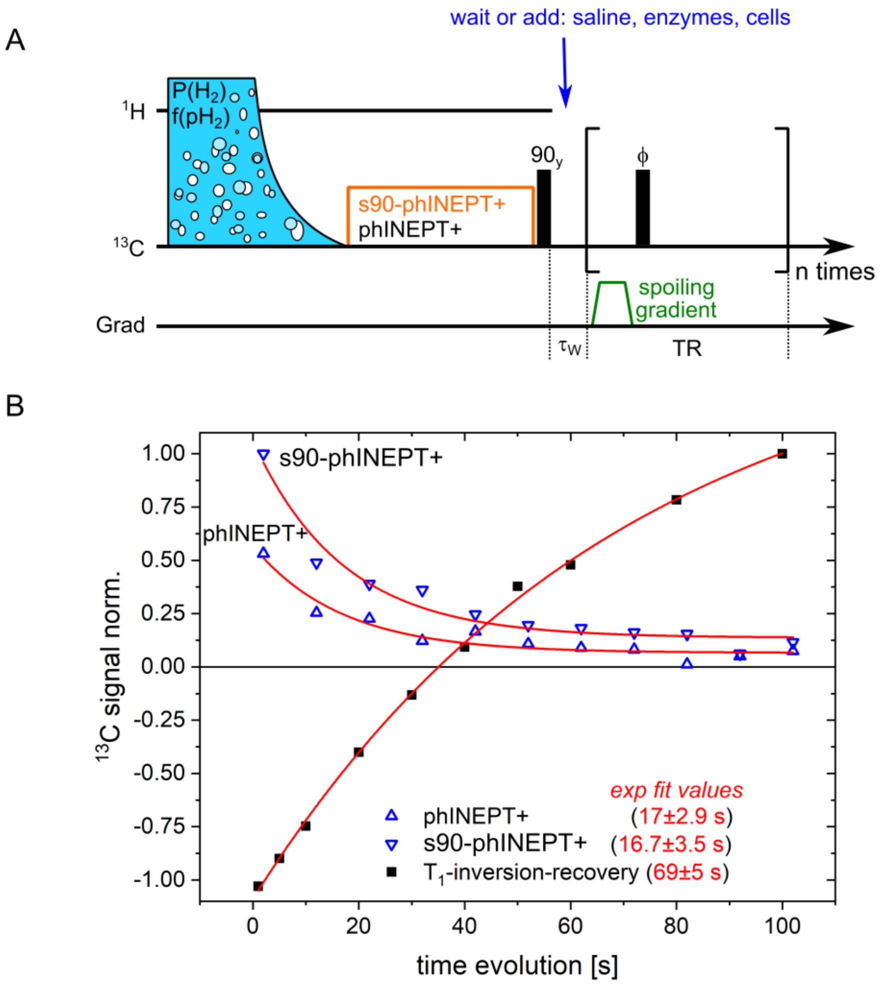

Figure S3. Refocused parahydrogen INEPT relaxometry and monitoring of chemical reaction scheme (A) and experiment (B). ^{13}C signal integrals of EA in polarization decay experiment (s90-phINEPT+ ▽, and phINEPT+ △) and T1-inversion recovery (■). The flipping angle ϕ was 30º, TR = 10 s, spoiling Z-gradient with the SMSQ10.100 shape: amplitude is 10 % from the maximum power with a duration of 2 ms. The INEPT signal is normalized on the first s90-phINEPT+ value. T1-inversion recovery integrals are normalized on the last value. The ^{13}C-integrals were fitted with an exponential decay function (red lines) and the corresponding decay values are given in the legend. The apparent lifetime of polarization is shorter because of consequent excitation with ϕ=30º. SAMBADENA[5] experiments will benefit from s90-phINEPT and its offsprings since it increase polarization at minimum costs. To use polarization in such experiments the polarization should be transferred to Z-axis before the consequent following manipulations with the hyperpolarized media (here it is indicated with words: "add saline, enzymes, cells" but the complete list can be continue by filtering, administration etc).

3. Evaluation of J-coupling constants

^{1}H NMR spectrum. ^{1}H spectrum of EA in chloroform-d was fitted in MestReNova 14.2.0 (**Fig S4**). The resulting J-coupling constants are given in **Fig 1** and **S4**.

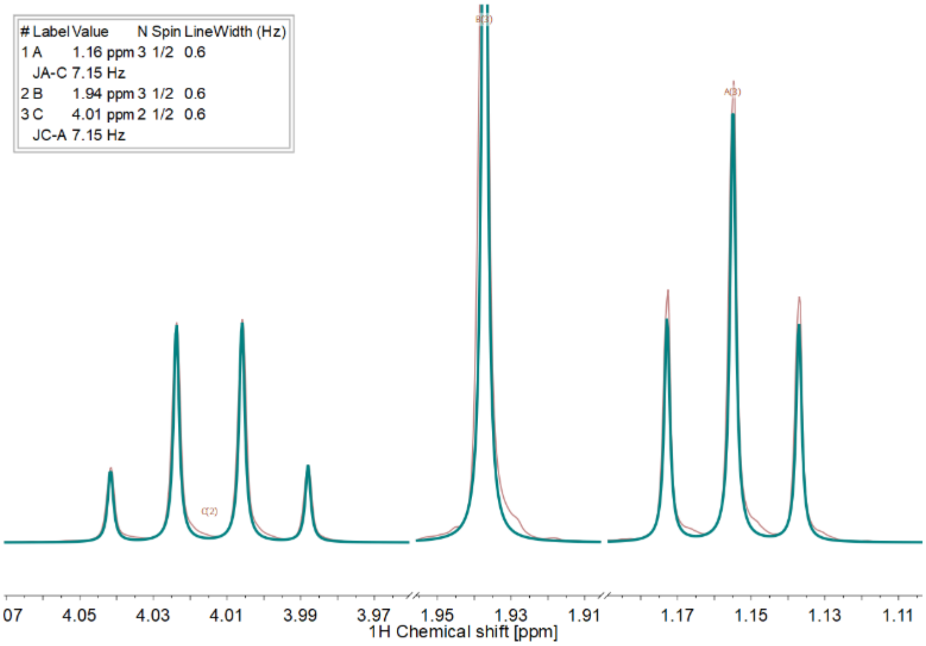

#	Label	Value	N	Spin	LineWidth (Hz)
1	A	1.16 ppm	3	1/2	0.6
	JA-C	7.15 Hz			
2	B	1.94 ppm	3	1/2	0.6
3	C	4.01 ppm	2	1/2	0.6
	JC-A	7.15 Hz			

Figure S4. Fitting of ^{1}H EA spectrum. The resulting chemical shifts and J-coupling constants are given in the table and used in the main text (**Fig 1).** The spectrum is measured in chloroform-d at 293 K after partial hydrogenation of VA.

^{13}C NMR spectrum. ^{13}C spectrum of [^{13}C-1]-EA (natural abundance) in chloroform-d was fitted in MestReNova 14.2.0 (**Fig S5**). The resulting J-coupling constants are given in **Fig 1** and **S5**.

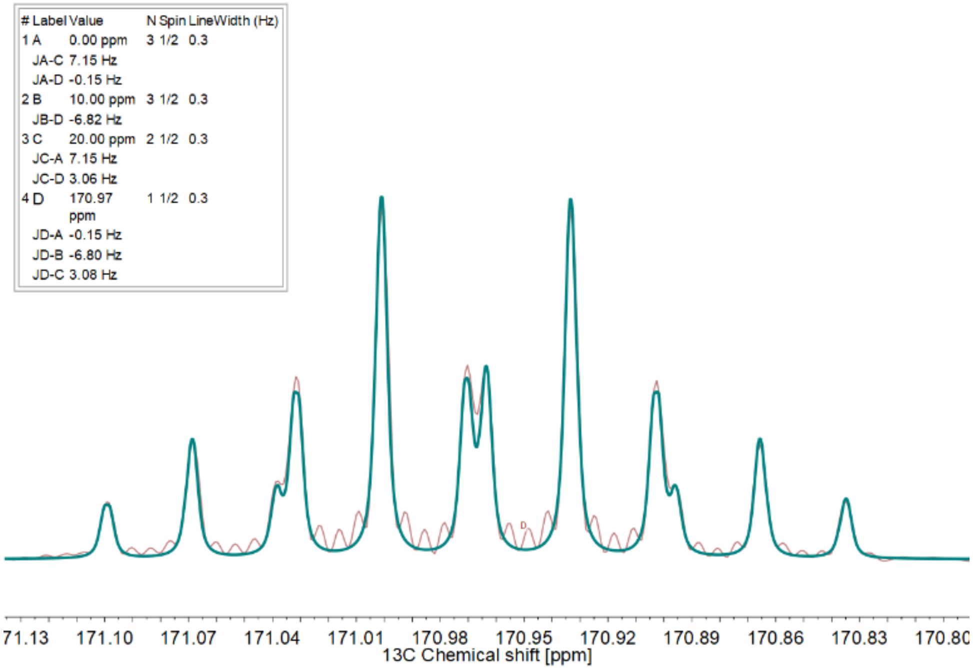

#	Label	Value	N	Spin	LineWidth (Hz)
1	A	0.00 ppm	3	1/2	0.3
	JA-C	7.15 Hz			
	JA-D	-0.15 Hz			
2	B	10.00 ppm	3	1/2	0.3
	JB-D	-6.82 Hz			
3	C	20.00 ppm	2	1/2	0.3
	JC-A	7.15 Hz			
	JC-D	3.06 Hz			
4	D	170.97 ppm	1	1/2	0.3
	JD-A	-0.15 Hz			
	JD-B	-6.80 Hz			
	JD-C	3.08 Hz			

Figure S5. Fitting of ^{13}C EA spectrum. The resulting chemical shifts and J-coupling constants are given in the table and used in the main text (**Fig 1).** The spectrum is measured in chloroform-d at 293 K after partial hydrogenation of VA.

4. Evolution of polarization

4.1. ^{1}H PASADENA spectra: FID(90$_x$)^{Mz}

Conventional, FID(90$_x$)^{Mz}, NMR experiment (single hard pulse and acquisition):

$$90_x - FID(t_{AQ}) \qquad \text{(eq S1)}$$

The initial state of the system is described by 100 % longitudinal magnetization, which is given by a $\frac{1}{2}(I_Z + S_Z)$ spin operators for s two spin system (AX-type). The evolution of this spin order in this experiment is following:

$$\frac{1}{2}(I_Z + S_Z) \xrightarrow{90_x} -\frac{1}{2}(I_Y + S_Y) \xrightarrow{p=-1} -\frac{i}{4}(I_- + S_-)$$

$$\xrightarrow{t_{AQ}(\omega_1 I_Z + \omega_2 S_Z)} \xrightarrow{\pi J t_{AQ} \cdot 2 I_Z S_Z} -\frac{i}{4}\left(I_- e^{i\omega_1 t_{AQ}} + S_- e^{i\omega_2 t_{AQ}}\right)\cos\left(\pi J t_{AQ}\right) + \cdots \qquad \text{(eq S2)}$$

Here, "$p = -1$" is a filter that reflects the fact that only -1 quantum coherences are observed.

Hence, the FID signal is following:

$$M^{tr}_{\mathrm{FID(90x)^{Mz}}}\left(t_{AQ}\right) = \left(-\frac{i}{8}\right)\left(e^{i\omega_1 t_{AQ}} + e^{i\omega_2 t_{AQ}}\right)\left(e^{i\pi J t_{AQ}} + e^{-i\pi J t_{AQ}}\right) \qquad \text{(eq S3)}$$

J-coupling constants define the shape of the spectrum; the number of equivalent spins gives the total integral. It is easy to show that the $M^{tr}_{\mathrm{FID(90_x)^{Mz}}}\left(t_{AQ}\right)$ for spins of A-type in A$_n$X$_m$ system is given by the function (**Fig S6**, net magnetization):

$$M^{tr}_{\mathrm{FID(spin\ A,\ 90_x)^{Mz}}}\left(t_{AQ}\right) = const \times n \times \cos^{\mathrm{m}}\left(\pi J t_{AQ}\right) \times e^{i\omega_A t_{AQ}} \qquad \text{(eq S4)}$$

$\cos^{m}(\pi J t_{AQ})$ results in the classical splitting of NMR spectral lines that follows the Pascal triangle rule.

4.2. ^{1}H PASADENA spectra: FID(selective-90$_x$)^{pH2}

A conventional PASADENA experiment is FID(45$_x$)^{pH2} and its difference with selective-90° pulse experiment, FID(selective-90$_x$)^{pH2} is discussed in the main text. The initial spin state of the system in a PASADENA experiment is given by $I_Z S_Z$ spin order (in fact $-I_Z S_Z$ but it is not essential here). During the FID(selective-90$_x$)^{pH2} sequence, the multiplet polarization evolves as follows:

$$I_Z S_Z \xrightarrow{(90_x)_I} -I_Y S_Z$$

$$\xrightarrow{p=-1} -\frac{i}{2} I_- S_Z$$

$$\xrightarrow{t_{AQ}(\omega_1 I_Z + \omega_2 S_Z)} \xrightarrow{\pi J t_{AQ} \cdot 2 I_Z S_Z} \frac{1}{4} I_- e^{i\omega_1 t_{AQ}} \sin(\pi J t_{AQ}) \qquad \text{(eq S5)}$$

Hence the FID signal is following:

$$M^{tr}_{\mathrm{FID(selective-90_x)^{pH_2}}}(t_{AQ}) = \left(-\frac{i}{8}\right) e^{i\omega_1 t_{AQ}} \left(e^{i\pi J t_{AQ}} - e^{-i\pi J t_{AQ}}\right) \qquad \text{(eq S6)}$$

This derivation (eq S1-S6) was given to show that the amplitudes are precisely the same as in $M^{tr}_{\mathrm{FID(90x)^{M_Z}}}$ but the shape of the spectral line is given by $\sin(\pi J t_{AQ})$ instead of cosine. Again, it is easy to show that $M^{tr}_{\mathrm{FID(selective-90_x)^{pH_2}}}(t_{AQ})$ for spin A in A$_n$X$_m$ system is given by (**Fig S6**, multiplet polarization):

$$M^{tr}_{\mathrm{FID(selective-90_x)^{pH_2}}}(t_{AQ}) = const \times n \times \sin(\pi J t_{AQ}) \times \cos^{m-1}(\pi J t_{AQ}) \times e^{i\omega_A t_{AQ}} \qquad \text{(eq S7)}$$

Note that the constant, $const$, is the same as in eq S4. Because the multiplicity in the spectrum with multiplet polarization is given now by $\sin(\pi J t_{AQ}) \times \cos^{m-1}(\pi J t_{AQ})$ instead of $\cos^{m}(\pi J t_{AQ})$, the partial cancelation of spectral lines (**Fig S6**) results in a smaller value of integrals. For the discussed system: AX_2, AX_3, A_2X_3, A_3X_2, it is two times smaller; other difference rises due to a different number of equivalent spins.

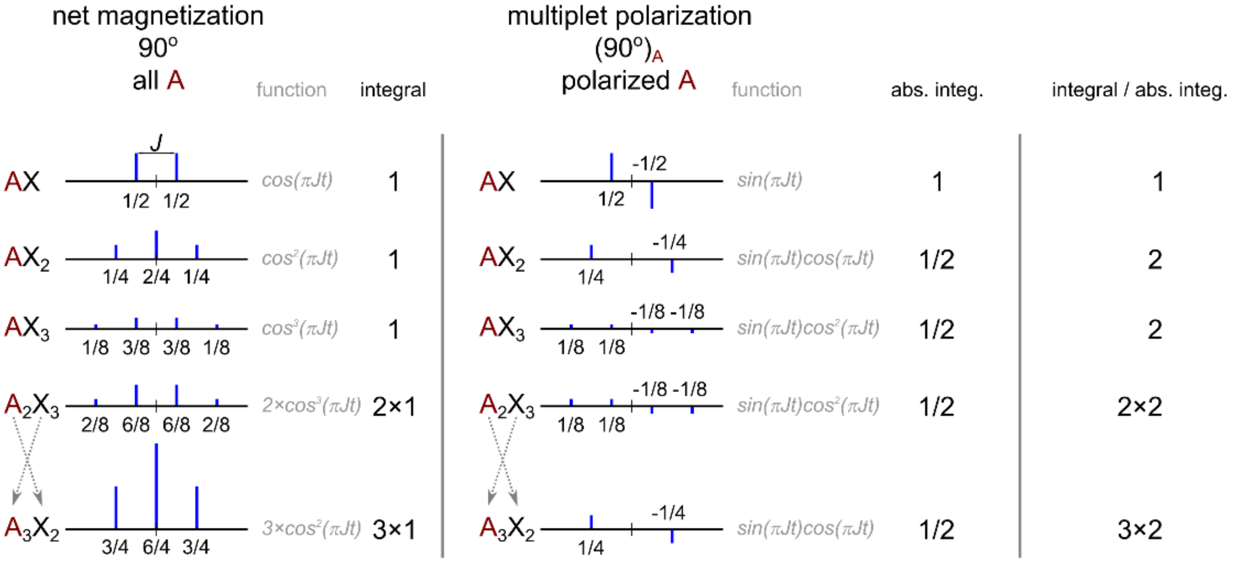

Figure S6. Line intensities in thermal (net magnetization) and PASADENA (multiplet polarization) spectra. It is convenient to assess the net magnetization by integrating the phased spectrum (here integral). Multiplet polarization on contrarily is evaluated as a difference of two integrals (absorptive minus emissive spectral lines) or by integrating an absolute spectrum (here abs. integ.).

4.3. Net polarization

It is straightforward to calculate the net polarization of spin A. First, one has to integrate polarized spectral lines of the spin of interest, I^{pol}. Second, one has to measure a thermal spectrum of the same molecule and integrate the same spectral lines, I^{th}.

The ratio of two integrals gives the signal enhancement and equal to the ratio of polarization levels:

$$\varepsilon = \frac{I^{pol}}{I^{th}} = \frac{P}{P^{th}} \qquad \text{(eq S8)}$$

Here, P is a current polarization and P^{th} is a thermal polarization. Polarization of a single spin in the high-temperature approximation is given by the

$$P^{th} = \frac{\hbar\gamma B}{2kT} = \frac{h\nu}{2kT} \qquad \text{(eq S9)}$$

Here, $\hbar$ and h are reduced and normal Planck constants, γ is a magnetogyric ratio, B is a magnetic field, ν is a resonance frequency of nucleus, k is Boltzmann constant and T is temperature.

The maximum absolute polarization value is 1. Therefore, maximum signal enhancement is

$$\varepsilon^{max} = \frac{1}{P^{th}} \qquad \text{(eq S10)}$$

From these three equations (eq S8-10), it follows that:

$$P = P^{th}\frac{I^{pol}}{I^{th}} = \frac{\varepsilon}{\varepsilon^{max}} = \varepsilon \times P^{th} \qquad \text{(eq S11)}$$

Note, the equations above (eq S8-11) are correct to the exact sign, which is not essential for the purpose of its evaluation. Using **eq S11** and values from **Tab S2**, the signal enhancements of ^{13}C at 9.4 T were calculated.

Table S2. Thermal polarization $\boldsymbol{P^{th}}$ and maximum signal enhancement $\boldsymbol{\varepsilon^{max}}$ for ^{1}H, ^{13}C and ^{15}N (the most important nuclei for PHIP) at 300 K and 1 T and 9.4 T magnetic field. Here the values of the following constants were used: $\gamma_{^1H} \cong 42.577$ MHz/T, $\gamma_{^{13}C} \cong 10.708$ MHz/T, $\gamma_{^{15}N} \cong -4.317$ MHz/T, $h \cong 6.6261 \cdot 10^{-34}$ J·s, $k \cong 1.38 \cdot 10^{-23}$ J/K.

Magnetic field	$P^{th}(^{1}\mathrm{H})$ $\boldsymbol{\varepsilon^{max}(^{1}\mathrm{H})}$	$P^{th}(^{13}\mathrm{C})$ $\boldsymbol{\varepsilon^{max}(^{13}\mathrm{C})}$	$P^{th}(^{15}\mathrm{N})$ $\boldsymbol{\varepsilon^{max}(^{15}\mathrm{N})}$
1 T: $\nu_{^1H}$ ≅42.576 MHz	$3.4 \cdot 10^{-6}$ $\mathbf{293,630}$	$8.56 \cdot 10^{-7}$ $\mathbf{1,167,500}$	$3.45 \cdot 10^{-7}$ $\mathbf{2,895,800}$
9.4 T: $\nu_{^1H}$ ≅400.21 MHz	$3.2 \cdot 10^{-5}$ $\mathbf{31,240}$	$8.05 \cdot 10^{-6}$ $\mathbf{124,200}$	$3.25 \cdot 10^{-6}$ $\mathbf{308,060}$

4.4. Multiplet polarization

It is not straightforward to calculate the signal enhancement and corresponding polarization level for a multiplet polarization as for net magnetization. Because of the partial cancelation of some spectral lines in the PASADENA spectrum (**Fig S6** – multiplet polarization), the polarized spectrum and thermal integrals do not match. As it is illustrated, the factor of 2 is needed for all spin systems but AX. In addition to that, the number of polarized spins and identical spins can also be different. Taking it all into account, we come up with the following equation for multiplet polarization:

$$mP = System\ Factor \times P^{th} \times \frac{abs.I^{pol}}{I^{th}/number\ of\ I\text{−}spins} = System\ Factor \times \frac{m\varepsilon}{\varepsilon^{max}} \qquad \text{(eq S12)}$$

Here $System\ Factor$ is 1 for an AX type of spin system and 2 in all other illustrated cases (**Fig S6**). $number\ of\ I - spins$ considers that only one proton is polarized, $abs.\,I^{pol}$ is an integral over the absolute spectrum or difference of integral over absorptive and emission lines, $m\varepsilon = \frac{abs.I^{pol}}{I^{th}/number\ of\ I\text{−}spins}$ is a multiplet enhancement. With this definition, mP reaches 100 % (or 1) when no losses occurred.

4.5. INEPT in symmetric and asymmetric ABX spin system

The application of phINEPT+ and s90-phINEPT+ to two three-spin systems of deuterated hydroxyethyl propionate (HEP) and ethyl acetate (EA) is demonstrated on **Fig S7**. These systems are different with respect to J-coupling constants. In the case of EA, only one of two hyperpolarized protons has coupling more than 5 Hz (7.1 Hz and -0.13 Hz, repsectively) while both coupling constants of HEP are of the same order (7.24 Hz, -5.62 Hz). In both cases, phINEPT+ provides a maximum of 50% polarization on the selected ^{13}C nucleus, while s90-phINEPT offers close to 100% ^{13}C-polarization.

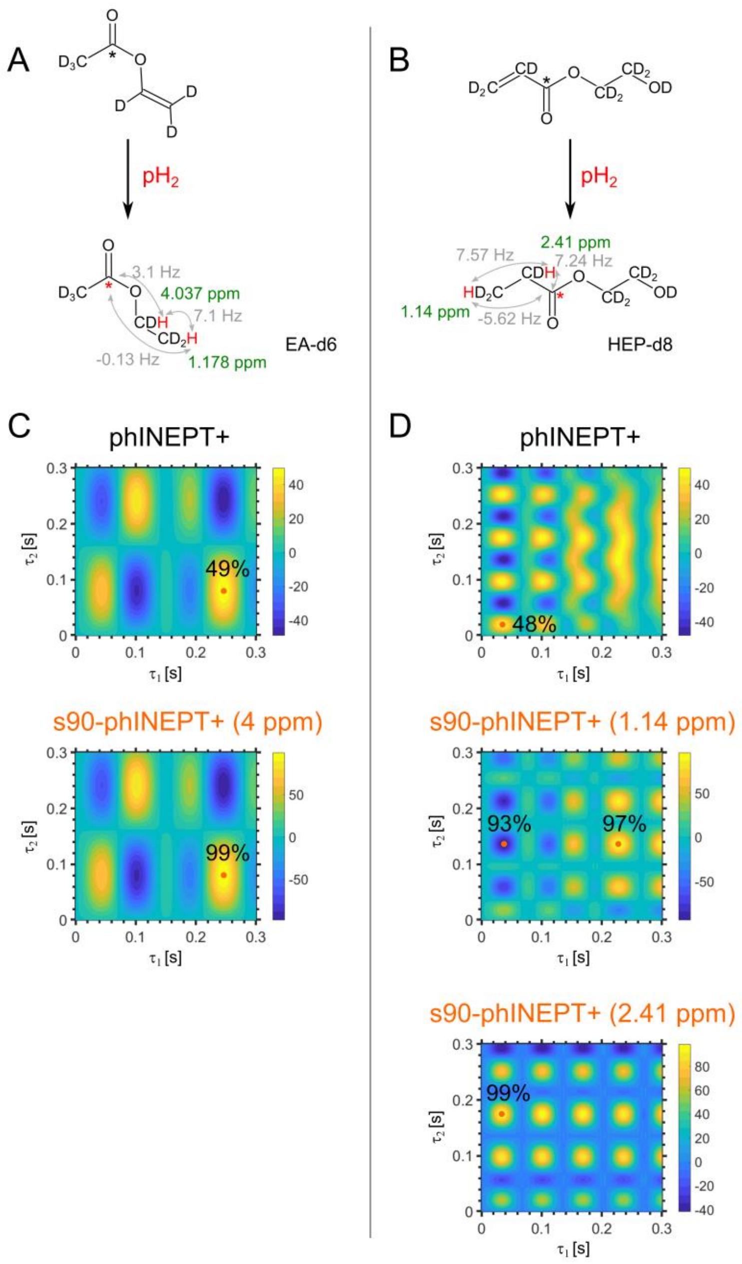

Figure S7. phINEPT+ performance in three-spin systems of deuterated ethyl acetate (EA-d6, A,C) and hydroxyethyl propionate (HEP-d8, B, D). Close to 100 % values are reached in s90-phINEPT+ and only ~50 % in phINEPT+. Polarization transfer efficiency after selective excitation of both protons of HEP is shown for s90-phINEPT+.

5. Supporting material references

(1) Pravdivtsev, A. N.; Hövener, J.-B. Simulating Non-Linear Chemical and Physical (CAP) Dynamics of Signal Amplification By Reversible Exchange (SABRE). *Chem. Eur. J.* **2019**, *25* (32), 7659–7668. https://doi.org/10.1002/chem.201806133.

(2) Pravdivtsev, A. N.; Skovpin, I. V.; Svyatova, A. I.; Chukanov, N. V.; Kovtunova, L. M.; Bukhtiyarov, V. I.; Chekmenev, E. Y.; Kovtunov, K. V.; Koptyug, I. V.; Hovener, J.-B. Chemical Exchange Reaction Effect on Polarization Transfer Efficiency in SLIC-SABRE. *J. Phys. Chem. A* **2018**. https://doi.org/10.1021/acs.jpca.8b07163.

(3) Pravdivtsev, A. N.; Hövener, J.-B. *MOIN Spin Library*; (www.moincc.de/method-development/mr/moin-spin-library) UKSH, University Kiel, 2018.

(4) Ellermann, F.; Pravdivtsev, A.; Hövener, J.-B. Open-Source, Partially 3D-Printed, High-Pressure (50-Bar) Liquid-Nitrogen-Cooled Parahydrogen Generator. *Magn. Reson.* **2021**, *2* (1), 49–62. https://doi.org/10.5194/mr-2-49-2021.

(5) Schmidt, A. B.; Berner, S.; Braig, M.; Zimmermann, M.; Hennig, J.; Elverfeldt, D. von; Hövener, J.-B. In Vivo 13C-MRI Using SAMBADENA. *PLOS ONE* **2018**, *13* (7), e0200141. https://doi.org/10.1371/journal.pone.0200141.